1 Introduction

Our concern is with Hamiltonian systems that by symmetry are reducible to one degree of freedom (or at least reducible to a large approximation). As a concrete example and as a case study for our approach we often consider a model for the spring–pendulum near one of its stronger resonances. For motivation and background the reader is referred to our extensive preface.

Focusing down further, we shall formulate the main goal of the present book. After reduction of the (approximating) Hamiltonian system by symmetry, we apply singularity theory to obtain transparent normal forms for the dynamical skeleton. For this we need coordinate transformations and reparametrizations, all of which can be obtained in an algorithmic way. It is our purpose to develop computer algebraic methods for this. Therefore, the emphasis lies on the *algorithmic methods*, especially in later chapters.

The earlier chapters are dealing with the translation between the context of dynamical systems on the one hand and that of the computer algebraic implementation of the singularity theory algorithms on the other hand.

Two reduction methods have been selected. These methods, dubbed the *planar reduction* [BCKV93] and *energy–momentum map* [Cus83, Dui84, Mee85] methods, both apply Birkhoff normal form transformation to obtain an (approximate) system with symmetry, and then proceed with reduction to a one degree of freedom system, in different ways. Algorithms for computing the reparametrizations involved are developed in chapter 4 onwards, and find application in both reduction methods in chapters 2 and 3. The algorithmic approach also enabled us to compute nondegeneracy conditions. Some of these were already found in [Dui84], also see [GMSD95], whereas certain others are rather hard to find by paper-and-pencil calculations.

As a byproduct of developing these algorithms we gain a deeper insight in the two reduction methods. Both methods are applied (and tested) on the concrete example of the spring–pendulum in a few strong resonances close to equilibrium. This enables us to make comparisons between the two methods, concerning their applicability and the strength of their dynamical conclusions. See Sect. 1.2 for a discussion.

Partly summarizing, we mention that the key ideas for making the planar reduction method algorithmic, and hence constructive, with suitable changes, are also applicable to the energy–momentum map method. In fact, this led to a

unifying approach to both methods, presented in chapters 6 and 7. The relevant notion for this unification is the standard basis, which deepened the understanding of the algorithms, and facilitated their derivation. Indeed, standard bases, and the Gröbner bases of which they are a generalization, prove to fit several ideas from both methods in a rather unexpected way.

1.1 A further setting of the problem

In this section, we explain the two reduction methods considered, by applying them to a simple two degree-of-freedom system. Our goal of explicitly computing coordinate transformations and reparametrizations, boils down to solving the so-called *infinitesimal stability equation*. In the context of polynomial rings, an efficient procedure based on Gröbner bases solves this equation. The two reduction methods motivate two different generalizations of this idea, leading *standard bases*.

1.1.1 The planar reduction method

The starting point is an article by Broer, Chow, Kim and Vegter [BCKV93], in which a two-step reduction method is used to find a polynomial model for a certain class of Hamiltonian dynamical systems. The reduction starts with a Birkhoff normalization. The resulting near $\mathbb{S}^1$ symmetry then is used to reduce to a planar one-degree-of-freedom system. Subsequently, right-equivalences (i.e., planar coordinate changes that are not necessarily symplectic) are used to find a polynomial and versal model system. Both steps are qualitative, in the sense explained above. On the one hand, to pull quantitative information through the Birkhoff normalization is feasible, as it was long known how to compute the associated (symplectic) conjugacy explicitly. On the other hand, for the versal deformation such explicit computations were, to our knowledge, not done before.

As said earlier, our aim is to see how much quantitative information about the original dynamical system could be mustered by computing the conjugacies along the lines of the planar reduction method. This program was presented in [BLV98] and carried out in detail in [BHLV98].

We now illustrate the planar reduction method by a simple example; for more details see [BCKV93, BCKV95]. Suppose we have a Hamiltonian living on $\mathbb{R}^4$ with a degenerate quadratic part, whose Hessian has corank 1. Then after Birkhoff normalization, truncation, and suitable time-reparametrizations, generically the following normal form results:

$$(1.1) \quad H(x_1, y_1, x_2, y_2) = \frac{1}{2}\left(x_1^2 + y_1^2\right) + \frac{1}{2}y_2^2 + \frac{1}{3}x_2^3 + g\left(\tfrac{1}{2}(x_1^2 + y_1^2), x_2, y_2\right),$$

with g containing all terms of degree 4 and higher. This system has an $\mathbb{S}^1$-symmetry (which is exact due to the truncation): rotation in the x_1, y_1-plane.

The semi-simple quadratic part $\lambda := \frac{1}{2}(x_1^2 + y_1^2)$ is the conserved quantity associated to this symmetry. We may treat λ as a parameter, and reduce to a planar system by ignoring the dynamics in x_1, y_1. This step is analogous to the reduction step in the Kepler problem. The resulting reduced system is

$$H^r(x_2, y_2, \lambda) = \frac{1}{2}y_2^2 + \frac{1}{3}x_2^3 + g(\lambda, x_2, y_2).$$

We now apply (non-symplectic) right transformations to normalize the system further. Since the system has one degree of freedom now, these transformations differ from symplectic ones by just a time reparametrization. The function that results when putting $\lambda = 0$ is called the *central singularity*. It may be brought into polynomial normal form $\frac{1}{2}y_2^2 + \frac{1}{3}x_2^3$ using the Splitting Lemma [BL75, Gib79, Mar82] and a classification theorem for singularities [Mar82, Sie74]. Hence we may assume that $g(0, x_2, y_2) \equiv 0$, that is, the system is now reduced to some deformation of the polynomial normal form.

The last step in the simplification process is finding a versal unfolding. To do this, we look at the tangent space to the orbit associated to the action of the group of right transformations on the central singularity. Locally, this tangent space may be identified with an ideal in the ring $\mathcal{E}_{x_2,y_2}$ of (germs of) functions depending on x_2, y_2. Generators of this ideal are $\partial/\partial x_2$ and $\partial/\partial y_2$ acting on the central singularity, resulting in the ideal $\langle x_2^2, y_2 \rangle$. As a real vector space, this is a codimension-1 subspace of the maximal ideal of $\mathcal{E}_{x_2,y_2}$ (also called the ring of (germs of) *potential functions*), and is complemented by, e.g., the 1-dimensional vector space spanned by the monomial x_2. The monomials chosen to complement the tangent space are called *deformation directions*. Adding the term μx_2 to the central singularity yields the versal unfolding:

$$H^u(x_2, y_2, \mu) = \frac{1}{2}y_2^2 + \frac{1}{3}x_2^3 + \mu x_2.$$

This happens to be the normal form of the *fold* catastrophe, one of the elementary catastrophes classified by René Thom [Tho72]. By the general theory it is known that H^r is conjugate to H^u by a reparametrization $\mu = \mu(\lambda)$, and a coordinate transformation (right-equivalence) ϕ of the x_2, y_2 depending on the parameter λ:

$$H^r(x_2, y_2, \lambda) = H^u(\phi(x_2, y_2, \lambda), \mu(\lambda));$$

we say that H^r is *induced* from H^u by ϕ and μ.

Up to this point we treated λ as an ordinary parameter, but actually it is a *distinguished* parameter, in the sense that it is a function on the 4-dimensional phase space. To reflect the special nature of λ in the normal form we restrict the class of allowed reparametrizations, so that changes in other parameters (which do not appear in our simple example) do not depend on λ, just as they do not depend on the phase variables x_2, y_2. Moreover, reparametrizations of λ are required to respect the zero level, which is natural since the 'action' λ is always positive. Following this idea (see also [BCKV93, BCKV95] and chapter 2), the final so-called *BCKV normal form* becomes
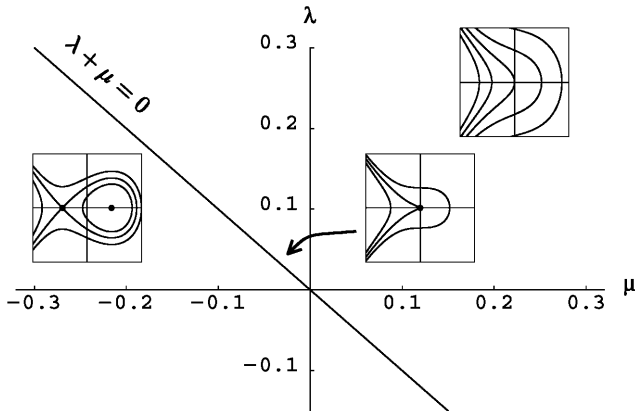
Fig. 1.1   Bifurcation diagram for (1.2): Hamiltonian saddle–node bifurcation

$$(1.2) \qquad H^B(x_2, y_2, \lambda, \mu) = \frac{1}{2}y_2^2 + \frac{1}{3}x_2^3 + (\mu + \lambda)x_2.$$

The bifurcation diagram is depicted in Fig. 1.1. We now return to the original question: How to compute this reparametrization and coordinate transformation? An algorithm due to Kas and Schlessinger [KS72] details how to compute such conjugacies and essentially reduces the problem to solving several instances of the so-called *infinitesimal stability equation*, which is related to the tangent space and the versal unfolding. For our example, this equation takes the form

$$(1.3) \qquad g(x_2, y_2) = \alpha_1(x_2, y_2)\frac{\partial F}{\partial x_2} + \alpha_2(x_2, y_2)\frac{\partial F}{\partial y_2} + \beta_1 x_2.$$

Here $F = \frac{1}{3}x_2^3 + \frac{1}{2}y_2^2$ is the central singularity; the expressions entering the infinitesimal stability equation are just the generators of the tangent space. The functions g are related to the $g(\lambda, x_2, y_2)$ above (in fact, they are the coefficients of $g(\lambda, x_2, y_2)$ expanded in powers of λ and the other parameters) and our task is to solve for functions α_i and real numbers β_i.

If the number of deformation parameters β_i is minimal, the β_i are uniquely determined, but in general the α_i are not. This is related to the fact that, for transformations inducing some deformation from a (uni)versal one, the *reparametrizations* are unique but the *coordinate transformations* generally are not. Algorithmically this is no problem – underdetermined systems are no more difficult to solve than uniquely determined ones.

Since we only want a finite part of the formal power series of the reparametrization and/or the coordinate transformation, solving the infinitesimal stability equation (1.3) is essentially a problem of finite-dimensional linear algebra. Though this solves our problem, two difficulties immediately emerge, one practical and another more fundamental in nature. On the practical side, the dimension of the matrices involved quickly becomes an issue: the number of monomials of

degree at most k increases rapidly with k. Since all matrix entries are symbolic expressions, solving the matrix equation soon becomes intractable – and many of such equations have to be solved.

More profound is the problem that the codimension of f, i.e., the number of deformation directions needed to complement the tangent space, can not be deduced straightforwardly from generators of this space. In other words, given generators of a formal power series ideal, it is in general not straightforward to find the highest order terms that determine its codimension as a real vector subspace of the ring.[1]

In the case of the *polynomial* ring, both problems are solved by Gröbner bases. Given arbitrary ideal generators, Buchberger's algorithm ([Buc65, BW93, CLO92], Sect. 6.4.1) yields generators of the same ideal that satisfy certain additional properties. These properties make computation of the codimension trivial, and can moreover be used to implement an efficient procedure for solving the infinitesimal stability equation (1.3) in the ring of polynomials. In [BHLV98] we developed methods suitable for formal power series rings, and applied it to the planar reduction method. We used the term *singularity Gröbner bases*, gleaned from [CW89]. Later it turned out that very similar ideas had already been developed, e.g., in [Mor82], using ideas of Hironaka (see [Hir64]). Hironaka coined the term *standard bases* for the analogue of Gröbner bases in formal power series rings. (Actually, Hironaka and Gröbner worked independently, with Hironaka's work preceding that of Gröbner by one year.)

1.1.2 The energy–momentum map

Next, we turn to the energy–momentum map reduction method, using the same example as before and also using the same terminology. The idea is to normalize a map from phase space to $\mathbb{R}^2$, whose two components are the Hamiltonian, and the conserved quantity λ associated to the $\mathbb{S}^1$-symmetry. (In this context, this quantity is referred to as the *momentum*.) This may be contrasted to the planar reduction method, which treats the Hamiltonian as the central object, and λ as a distinguished parameter. Since both the Hamiltonian and λ are conserved, fibers of the energy–momentum map are dynamically invariant.

In our example the system has two degrees of freedom. Then, after dividing out the symmetry, the fibers are 1 dimensional, so that they correspond to *orbits* of the system (though without time-parametrization). Since the set of fibers smoothly deforms when the energy–momentum map is subjected to smooth left–right transformations, it is natural to use these equivalences to bring the map in normal form.

Assume the system is already in (truncated) Birkhoff normal form (1.1), so that it has an exact $\mathbb{S}^1$-symmetry. We divide out this symmetry by going to

---

[1] However, it should be noted that in our particular example, the computation of the codimension can be easily handled by *ad hoc* methods. This is not true anymore for the reduction method that uses the energy–momentum map.

invariant coordinates. In this case $\rho_1 := \frac{1}{2}(x_1^2 + y_1^2)$, x_2 and y_2 together form a Hilbert basis (minimal set of generators; see [CLO92, Gat00, Hil93]) of the space of $\mathbb{S}^1$-invariant functions. In these coordinates, the energy–momentum map $\boldsymbol{E} : \mathbb{R}^3 \to \mathbb{R}^2$ takes the form

$$\boldsymbol{E} : (\rho_1, x_2, y_2) \mapsto (\; H \;,\; \lambda \;) = \left(\; \rho_1 + \frac{1}{2}y_2^2 + \frac{1}{3}x_2^3 + g(\rho_1, x_2, y_2) \;,\; \rho_1 \; \right).$$

In order to compute $\boldsymbol{E}$'s normal form, we have to know the tangent space of its orbit under left–right equivalences (B, A). These equivalences form a *group*, with operation $(B', A') * (B, A) = (B' \circ B, A \circ A')$, and deform $\boldsymbol{E}$ in the following way:

$$(B, A) : \quad \boldsymbol{E} \mapsto B \circ \boldsymbol{E} \circ A,$$

where B deforms the range of $\boldsymbol{E}$, and A is $\mathbb{S}^1$-equivariant. Generators of $\mathbb{S}_1$-equivariant vector fields (on $\mathbb{R}^4$) are $\frac{1}{2}(x_1 \frac{\partial}{\partial x_1} + y_1 \frac{\partial}{\partial y_1})$, $y_1 \frac{\partial}{\partial x_1} - x_1 \frac{\partial}{\partial y_1}$, $\frac{\partial}{\partial x_2}$ and $\frac{\partial}{\partial y_2}$; in invariant coordinates the first becomes $\rho_1 \frac{\partial}{\partial \rho_1}$ whereas the second vanishes. (It follows that, in invariant coordinates, $\mathbb{S}^1$-equivariance of A boils down to the requirement that the subspace $\rho_1 = 0$ be invariant.) We want to compute the tangent space to the orbit of $\boldsymbol{E}$ under such transformations. It turns out that this tangent space is not an ideal, as it was in the previous example. This makes computing the codimension technically difficult; see, e.g., the remark in [Mar82, p. 183]. These difficulties only become more profound when explicit reparametrizations are computed. In order to show what form the tangent space takes, we need to go into some detail here.

Working with maps is less convenient than working with functions, so we try to reduce to the latter case. A small computation shows that the projection of the tangent space onto the second component is surjective; hence, we may restrict to left–right transformations that leave $\boldsymbol{E}$'s second component invariant, and compute the tangent space of the orbit of $\boldsymbol{E}$'s *first* component under such transformations. (See Sect. 3.2.3 for an elaboration of this argument.) We call this the *reduced tangent space*.

Let us denote coordinates on the range of $\boldsymbol{E}$ by ζ_1, ζ_2. Tangent vectors to the space of left–right transformations (B, A) are pairs of vector fields, on $\mathbb{R}^2 \ni (\zeta_1, \zeta_2)$ and $\mathbb{R}^3 \ni (\rho_1, x_1, x_2)$. One class of tangent vectors leaving the second component of $\boldsymbol{E}$ invariant is generated by the following:

$$\left(0 \;,\; h_1(\rho_1, x_2, y_2) \frac{\partial}{\partial x_2} \right) \quad \text{and} \quad \left(0 \;,\; h_2(\rho_1, x_2, y_2) \frac{\partial}{\partial y_2} \right),$$

namely those generating right-transformations that leave ρ_1 invariant altogether. (Here the h_i are arbitrary functions of ρ_1, x_2, y_2.) Another class is formed by vectors generating left-transformations that leave the second component unchanged:

$$\left(f_1(\zeta_1, \zeta_2) \frac{\partial}{\partial \zeta_1} \;,\; 0 \right).$$

Here f_1 is an arbitrary function of two variables. The third class of vectors generate left–right transformations, interacting in such a way that their *combined* action leaves $\boldsymbol{E}$'s second component invariant:

$$\left(-\zeta_1 f_2(\zeta_1,\zeta_2)\frac{\partial}{\partial\zeta_2}\ ,\ f_2(H,\rho_1)\boldsymbol{\alpha}\right)\ \text{and}\ \left(-\zeta_2 f_3(\zeta_1,\zeta_2)\frac{\partial}{\partial\zeta_2}\ ,\ f_3(H,\rho_1)\rho_1\frac{\partial}{\partial\rho_1}\right).$$

Again the f_i are arbitrary functions, and $\boldsymbol{\alpha}$ a vector field on $\mathbb{R}^3$ such that $\boldsymbol{\alpha}\rho_1 = H$. Applying these tangent vectors to the map $\boldsymbol{E}$ and projecting to the first component, the reduced tangent space (to the map $\boldsymbol{E}$) becomes

$$\left\{h_1\frac{\partial H}{\partial x_2}+h_2\frac{\partial H}{\partial y_2}+f_1(H,\rho_1)+f_2(H,\rho_1)\boldsymbol{\alpha}H+f_3(H,\rho_1)\frac{\partial H}{\partial\rho_1}\right\}\subseteq\mathcal{E}_{\rho_1,x_2,y_2},$$

where $\mathcal{E}_{\rho_1,x_2,y_2}$ is the set of functions depending on ρ_1, x_2, y_2. Observe that this is not, indeed, an ideal over $\mathcal{E}_{\rho_1,x_2,y_2}$.

To complete the discussion of this example, we note that the first two terms together span the tangent space related to the right-transformations only. Since in the planar reduction example this alone was enough to get to a codimension 1 singularity, the present tangent space has at most codimension 1. In fact, it is easy to see that x_2 is not in the tangent space, so that the codimension is indeed 1. Normal form and versal unfolding are identical to the previous example; see Fig. 1.1 for bifurcation curves.

This completes the *qualitative* analysis. We now have a versal model of the system; it remains to compute coordinate transformations inducing the actual (Birkhoff-normalized) system from the versal model. One ingredient, Kas and Schlessinger's algorithm, may be moulded to fit the present situation quite straightforwardly, the only technical complication being the step from the reduced tangent space back to the actual tangent space of the mapping. As in the planar reduction case, Kas and Schlessinger's algorithm requires solutions to the infinitesimal stability equation. To compute these efficiently is more difficult.

In contrast to the planar reduction method, which uses right-transformations as equivalences and consequently yields an ideal as tangent space, currently the tangent space has a more complicated structure, since it is a combination of an ideal and a module over an algebra. Our initial idea was that once a suitable generalization of a Gröbner basis for algebras (instead of ideals) was found, integration of the various parts would be straightforward. The required generalization was known in the literature as *canonical subalgebra basis* [Stu93, Stu96] or *SAGBI basis* [Vas98].

1.1.3 Standard bases

However, applying these ideas to our example of the left–right tangent space turned out to be difficult. For some time we tried to resolve the difficulties in an *ad hoc* manner, resulting in several almost-identical algorithms and constructions.

From these, we could finally pinpoint the similarities and differences between the various constructions ranging from Gröbner bases, standard ideal bases, canonical subalgebra bases to analogous bases for left–right tangent spaces. All of these constructions could be put in a general framework, built around two central objects called *standard maps* and *standard bases*. Viewing these constructions as instances of a more abstract construction greatly clarified the situation. It suggested transparent notation, and eliminated the near-similar proofs.

A central role is played by the *standard map theorem*, theorem 6.10. It was inspired by Greuel's proof [GP88] of the ordinary Gröbner basis theorem, which exploits an idea by Schreyer [Sch91] for computing the module of syzygies of ideal generators. In contrast to the usual proofs, Greuel's proof uses the ideal structure only superficially, which facilitated the generalization to other algebraic structures. Another object borrowed from Greuel that, with a small modification, proved very useful, is the *normal form map*. This map plays the role of a 'lazy' division algorithm, analogous to the normal form algorithm for Gröbner bases. (Incidentally, this map is unrelated to Birkhoff's normal form procedure.) The map is required to satisfy only mild conditions, and exists under very general assumptions on the base ring and term ordering: For the polynomial ring, it exists whenever the term order is a well-order, whereas for the formal power series ring, the term order should be a reversed well-order. For details also see [Lun99b]

1.2 Sketch of the results

We briefly present our results, splitting the presentation into two parts. First we discuss the results obtained in applying the algorithmic methods to the spring–pendulum in chapters 2 and 3. Second we discuss the algorithmic methods themselves, as far as they are new.

1.2.1 Reduction methods

Both reduction methods for Hamiltonian systems around an equilibrium point and close to resonance, elaborated in chapters 2 and 3 respectively, have the same goal, namely describing the local dynamics of the system.

Remark 1.1. To be precise, we describe the dynamics of the *Birkhoff normalized* $\mathbb{S}^1$-symmetric system, which differs from the original system by a smooth coordinate transformation and a flat (generally) non-symmetric perturbation. The perturbation problem involved here is ignored in this study, for some remarks and references see the preface. Since we focus on an integrable approximation, we do not find chaotic dynamics in our final model system. However, since the the real system is a flat perturbation of the model system, the difference is extremely small for modest energies (i.e., for modest deviations from the equilibrium) so that our approximation is very good. This conclusion is confirmed by numerical

experiments. In two degree of freedom systems we can say even more, see the introduction to chapter 2.

Since both reduction methods differ considerably in their approach, but still have the same aim, it is interesting to compare their results. We chose to apply both methods to the spring–pendulum system in $1:2$ resonance. This particular resonance was chosen because both methods are able to handle it. In chapters 2 and 3 we do a part of the analysis for other resonances as well, but only the $1:2$ case is carried out fully.

1.2.2 The planar reduction method

Our spring–pendulum model (see Fig. 2.1 in section 2.3.1) has various physical parameters, like pendulum length and mass, spring constant *etc.* For simplicity we use the coefficients a_i of the Taylor expansion of the system's Hamiltonian as parameters, see (2.7). The Hamiltonian has two degrees of freedom, and can be brought in the form

$$(1.4) \qquad H^0(x_1, y_1, x_2, y_2) := \frac{x_1^2 + y_1^2}{2} + a_1 \frac{x_2^2 + y_2^2}{2} + h.o.t.$$

Here the x_i are configuration variables and the y_i momentum variables. The parameter a_1 determines the frequency ratio of the two harmonic oscillators of the quadratic truncation (or linear truncation of the vector field). We shall assume we are close to the $1:2$ resonance, i.e., $a_1 \approx 1/2$.

Next, we apply the Birkhoff normalization procedure, and we truncate. The result is an $\mathbb{S}^1$ symmetry, and a conserved quantity λ. Regarding λ as a parameter and dividing out the symmetry, we get a planar system in the variables x, y. The relation between the original variables x_1, y_1, x_2, y_2 and the planar variables x, y is as follows: On the section $y_2 = 0$ we have $x = x_1$ and $y = y_1$, modulo higher order terms. A singularity theory normalization of the planar system, as explained in Sect. 1.1, yields the following versal family:

$$(1.5) \qquad H^u(x, y) = x(x^2 + y^2) + u_1 x + u_2 y^2,$$

the $\mathbb{Z}_2$-symmetric hyperbolic umbilic D_4^+, see Proposition 2.13. Here u_1 and u_2 are deformation parameters. (The $\mathbb{Z}_2$ symmetry, originating from the system's reversibility, and acting as $(x, y) \mapsto (x, -y)$, is the reason that no deformation term $u_3 y$ is needed.) The family defines a Hamiltonian system in x and y which is equivalent (i.e., conjugate modulo time reparametrizations) to the planar reduction.

We here reproduce the bifurcation diagram, Fig. 2.5, in Fig. 1.2. It depicts the phase diagrams that occur in the planar system (1.5); the shaded parts correspond to inaccessible regions either in the phase or parameter plane. (They occur because of singularities in the coordinate transformations; points in the inaccessible regions correspond to imaginary values of parameters or phase variables.)
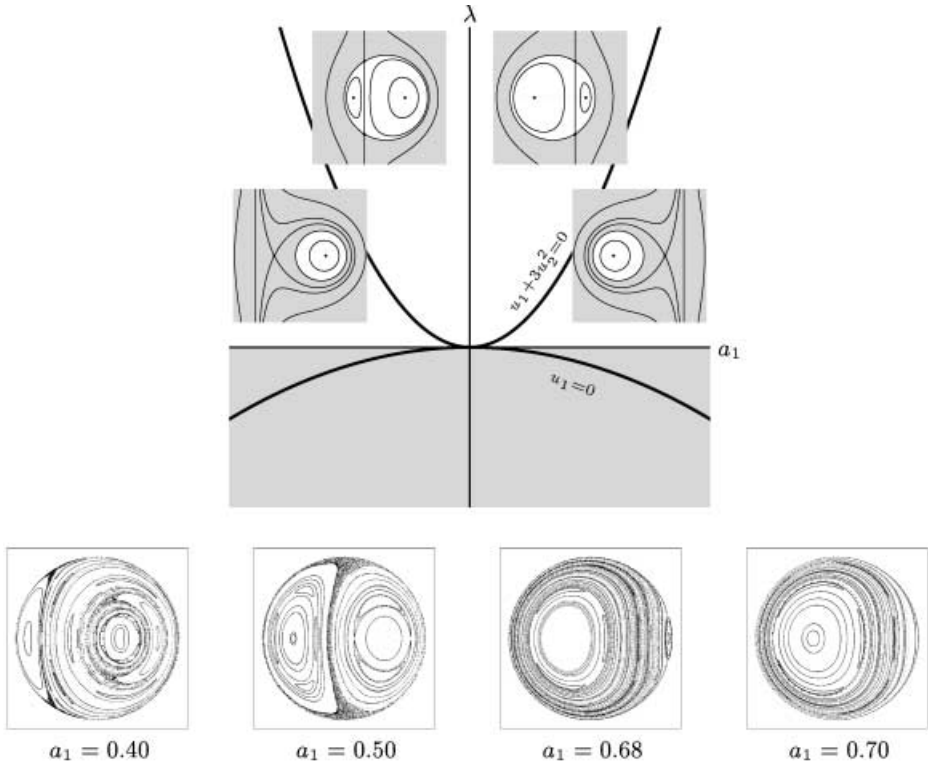
Fig. 1.2 Bifurcation diagram for the model (1.5), and numerical iso-energetic Poincaré maps. Grey areas correspond to non-physical states or parameter settings. Note the similarities between the bifurcation diagram and the Poincaré maps, as well as the effect of nonintegrability in the latter.

In the family (1.5) two curves of bifurcations occur, $u_1 = 0$ and $u_1 + 3u_2^2 = 0$ (see Sect. 2.3.3). The former lies in an inaccessible region, whereas the latter corresponds to a line of Hamiltonian pitchfork bifurcations. With the help of explicit expressions for the normalizing transformations, we can pull back this curve to original parameters. The result is the following bifurcation curve:

$$(1.6) \qquad \lambda = \frac{(1 - 2a_1)^2}{64a_2^2} + \frac{(a_2^2 - a_4)(1 - 2a_1)^3}{128a_2^4} + O((1 - 2a_1)^4),$$

see Proposition 2.18. Here the a_i are coefficients of the original Hamiltonian (1.4) or (2.7), and λ is the conserved quantity. An expression for the latter in original phase space variables can be computed using the Birkhoff normalization procedure; see (2.8). Combining (1.6) and (2.8), the bifurcation equation can be checked by numerical simulations of the Poincaré map. The results may be found in table 2.2 and Fig. 2.3.

The final step involves a versal model under a restricted equivalence class, the so-called BCKV-restricted morphisms; see [BCKV93, BCKV95, BHLV98] as well as Sect. 2.2.7. This class distinguished three levels of variables, namely phase space variables, distinguished parameters and ordinary parameters. The distinguished parameters are parameters for the final model, but originate from phase space, as conserved quantities. These morphisms allow transformations of distinguished parameters to depend on both kinds of parameters, but disallow those of ordinary parameters to depend on distinguished ones. This ensures that reparametrizations applied on the reduced family may be pulled back to the original phase space without mixing parameters and phase space variables. This results in a model given in Proposition 2.16. It gives rise to the same qualitative behavior, i.e., bifurcations, but with an additional nondegeneracy condition; see also remark 2.17 in Chapter 2.

Other resonances The planar reduction method cannot be used for resonances $p : q$ with q odd. The reason is that the iso-energetic 3-torus on which the system lives has two singular points, corresponding to simple periodic motion. When reducing this to the plane, one of these is mapped to a circle, here referred to as the *singular circle* (see remark 2.5 and Sect. 2.3.3). It is then essential that the function is smooth at this circle, which only happens for q even (see Proposition 2.4).

Having done the 1:2 case, the next case to consider is the 1:4 resonance. Again from Proposition 2.4 one can (correctly) guess that the versal family has a central singularity of the form

$$\text{(1.7)} \qquad \alpha(x^2 + y^2)^2 + \beta x(x^2 + y^2)^2.$$

With respect to equivalence via $\mathbb{Z}_2$-equivariant planar right-transformations, this function has infinite codimension. This seems to imply that the system in $1 : 4$ resonance is highly degenerate, and that small perturbations can spawn many qualitatively different kinds of dynamics. This is not the case: Both the odd-resonance problem and this high-codimension phenomenon result from perturbing within the class of $\mathbb{Z}_2$-invariant planar functions.

If a perturbation is applied to the *original* system, then after Birkhoff normalization this perturbation is 'projected' inside the class of functions generated by the $\mathbb{S}^1$-invariants $x^2 + y^2$, λ, and one of

$$(x^2 - y^2)(x^2 + y^2)^A(x^2 + y^2 - \lambda/C)^B \quad \text{and} \quad x(x^2 + y^2)^A(x^2 + y^2 - \lambda/C)^B.$$

(Here A, B and C are integers depending on p and q, see Proposition 2.4.) To require (1.7) to be versal with respect to arbitrary ($\mathbb{Z}_2$-symmetric) planar perturbations is to ask for more than we need. The class of equivalences, arbitrary $\mathbb{Z}_2$-equivariant right transformations, is also larger; however, the net effect is still that (1.7) has infinite codimension with respect to this class of perturbations.

In the next section we consider another reduction method, which uses equivalences that respect the $\mathbb{S}^1$-symmetry. It turns out that this method does find finite codimension models for higher order resonances.
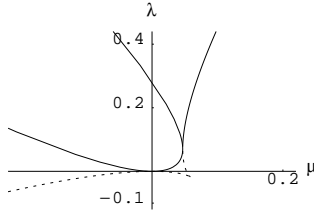
Fig. 1.3   Bifurcation curves for (1.8), with parameters $a = \frac{1}{4}$ and $b = \frac{1}{3}$.

1.2.3 The energy–momentum map method

As with the planar reduction method, we use the coefficients of the Taylor expansion of the spring–pendulum system (equation 2.8) as basic parameters, and again assume that we are close to the $1 : 2$ resonance, i.e., $a_1 \approx 1/2$. As normal form for the energy–momentum map we find

$$(1.8) \qquad (H^\mu, \lambda) = \left(\frac{1}{2}\rho_1 + \left(\frac{1}{4} + \mu \right) \rho_2 + a\psi + b\rho_1\rho_2 \;\;,\;\; \frac{1}{2}\rho_1 + \frac{1}{4}\rho_2 \right),$$

see (3.12). Here λ is the conserved quantity associated with the $\mathbb{S}^1$ symmetry, which in this case is just the quadratic part of H. In (1.8), a and b are coefficients, μ the deformation parameter, also called the *detuning parameter*, and ρ_1, ρ_2, ψ are three $\mathbb{S}^1$-invariants that form a Hilbert basis for the $\mathbb{S}^1$-symmetric functions. They have a relation which is implicit from the following connection with the coordinates x, y used in the planar reduction case:

$$\rho_1 = x^2 + y^2, \quad \rho_2 = 4\lambda - 2(x^2 + y^2), \quad \psi = 2x(2\lambda - x^2 - y^2).$$

 The bifurcations of this model, i.e., the μ values for which the number of relative equilibria changes, form a parabola and a cubic curve in the λ, μ plane; see Fig. 3.4 which is reproduced here as Fig. 1.3. Figure 1.4 displays the bifurcation sequence for fixed, small and positive λ, and increasing μ. (We used the Poincaré section transversal to the long periodic orbit; for the other Poincaré section see Fig. 3.5.) The parameter μ is related to the quantity $1 - 2a_1$, which measures the deviation from the $1 : 2$ resonance. Three bifurcations occur as μ increases, hence its name of 'detuning parameter'. Two of those are pitchfork bifurcations corresponding to the parabola and occur for small μ. The other is a saddle–node bifurcation and occurs for finite μ, in the limit as λ tends to 0. To pull back the bifurcation curve to original coordinates, the λ-level at the bifurcation points need to be computed, as in contrast to the planar reduction method, λ-levels are not preserved by the left–right transformations. The result is

$$(1.9) \qquad \lambda = \frac{(1 - 2a_1)^2}{64a_2^2} + \frac{(2a_2^2 + 6a_3 - a_4 - 2a_5)(1 - 2a_1)^3}{128a_2^4} + O(|1 - 2a_1|^4)$$
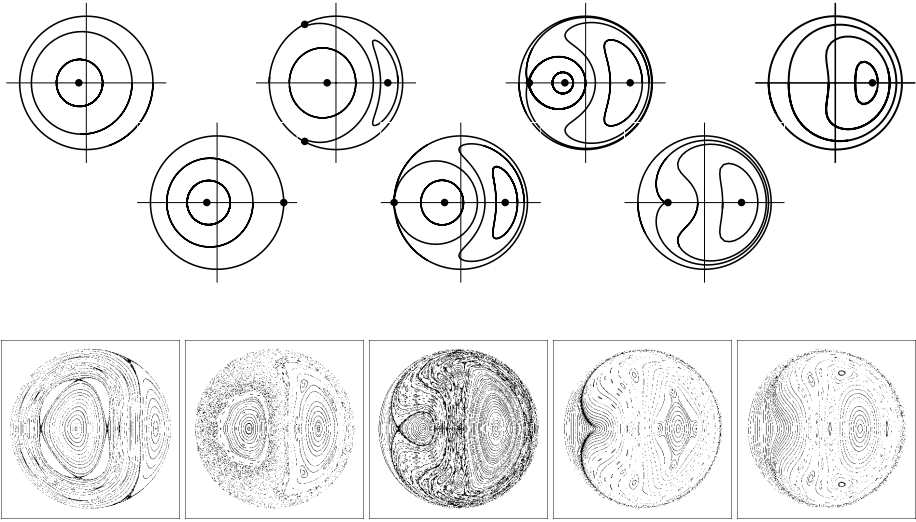
Fig. 1.4   Bifurcations of the energy–momentum map normal form around the 1 : 2 resonance for small increasing μ (left to right), crossing the solid curves of Fig. 1.3 three times, resulting in four structurally stable phase diagrams (top row). Below are some corresponding Poincaré sections obtained by numerical integration.

for the pitchfork bifurcation; see Sect. 3.4.3. Here λ is the integral of the system, see (2.8). The saddle–node bifurcation occurs outside the origin, and for $O(1)$ values of the detuning parameter $1 - 2a_1$; see (3.19) in Sect. 3.4.1, which means that a formal power series approximation of a coordinate transformation cannot be used to approximate the bifurcation curve in original parameters.

Remark 1.2. The saddle–node bifurcation away from $(\lambda, \mu) = (0, 0)$, however relevant it may be for the physical model and numerical simulations under study, is outside the present theoretical consideration. A more careful analysis of the model will be needed to study this bifurcation.

As can be seen from (1.8), the versal model has 1 parameter, so it has codimension 1. It therefore seems that this model has lower codimension than the planar model of the previous section. However, this difference is superficial and due to accountancy only. Indeed, the planar reduction method regards λ as a (distinguished) parameter, whereas with the present energy–momentum method λ is part of the map. (Earlier computations on the energy–momentum map used only right-transformations, which resulted in a codimension 2 model, see [Dui81].)

Other resonances   The methods used for the 1:2 resonance can be applied more generally. The 1:4 resonance (see Sect. 3.3.3) results in a versal family with 2 parameters (or 3 if λ is counted as a parameter). Apart from small differences

in the formulas for the nondegeneracy conditions, the results agree with those in [Dui84].

The computations for the 1:3 resonance are rather involved. The complexity is evidenced by the lengthy expressions for the nondegeneracy conditions; see Sect. 3.3.2. For sketches of the bifurcation diagrams for both of these resonances, as well as for the cases $p : q$ with $|p| + |q| > 4$, e.g., see [Dui84, GMSD95].

Other interesting resonances are the 1:1 and 1:-1 cases. In contrast to higher order resonances, the sign (referring to the positive-definite and indefinite cases, respectively) makes a great difference here. In [Mee85] the 1:-1 resonance is analyzed in detail. Cotter [Cot86] analyzes the semisimple 1:1 resonance. It would be interesting to apply our methods to these cases, in order to obtain explicit bifurcation curves. This is relevant for systems like the restricted three-body problem around Routh's mass ratio, see, e.g., [DH68, Mee85, MH92, MS71, Rou75].

Remark 1.3. An interesting example to apply the present techniques to, is the restricted three-body problem. Like the spring–pendulum, also this system has two degrees of freedom. The main difference with the former is that it has a hyperbolic instead of elliptic equilibrium, leading to different 'allowed zones' in the bifurcation pictures.

1.2.4 Standard bases

Gröbner bases enabled the algorithmic treatment of polynomial ideals. We now briefly sketch the ideas behind it, in order to give a heuristic introduction to standard bases and to indicate the relationship between Gröbner and standard bases.

Given any order on the monomials (satisfying some conditions that we ignore for now), a Gröbner basis is a basis $\{h_1, \ldots, h_n\}$ for an ideal $I = \langle h_1, \ldots, h_n \rangle$ such that every monomial that occurs as *leading monomial* of an element of I, according to the monomial order, is a multiple of the leading monomial of some h_i. In a precise sense, a Gröbner basis is to its ideal what a matrix in row-echelon form is to its image, when regarded as a linear operator. To be specific, for a matrix A in row-echelon form it is easy to determine the codimension of its range, and for a Gröbner basis it is similarly easy to determine the codimension of the corresponding ideal regarded as a real vector subspace of the ring in which it lives. Also, for such a matrix, solving the equation $Ax = b$ for x is straightforward, and this corresponds to the existence of a so-called *normal form map* (or algorithm) solving a similar equation for ideals; in particular, it solves the ideal membership problem. Standard bases are a generalization of Gröbner bases to algebraic structures other than ideals – and to a lesser extent, also to other base rings than the polynomial ring. They are best explained using Fig. 6.3 which is reproduced here as Fig. 1.5. For the case of Gröbner bases, R is the polynomial ring, $M = R^n$ and Ψ is the R-module homomorphism given by $(a_1, \ldots, a_n) \mapsto \sum a_i h_i$, so that the image of Ψ is the ideal I. The map $\widetilde{\Psi}$ maps $(a_1, \ldots, a_n)$ to $\sum a_i \, \mathsf{LT} \, h_i$; here $\mathsf{LT} \, h_i$ is the leading term of h_i, so that the image
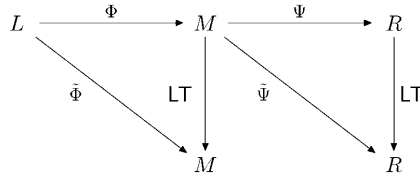
Fig. 1.5 Diagram for the standard map theorem. Under computable conditions on Φ and Ψ, the sequence $L \xrightarrow{\Phi} M \xrightarrow{\Psi} R$ is exact and Φ, Ψ are standard maps.

of $\widetilde{\Psi}$ are all multiples of leading monomials of the ideal generators h_i. Now the question of $\{h_i\}$ being a Gröbner basis can be rephrased as: Is it true that

$$\mathsf{LT}\,\mathrm{Im}\,\Psi = \mathrm{Im}\,\widetilde{\Psi} \quad ?$$

(Here LT applied to a set is the span of the $\mathsf{LT}\,f$, where f ranges over the set.) If equality holds, the map Ψ is called a *standard map*, and the basis $\{h_i\}$ a *standard basis*. For ideal bases, the question whether the associated map Ψ is a standard map is settled by looking at S-polynomials (for *syzygy polynomials*), combinations of ideal generators that cancel leading terms. In other words, S-polynomials are the images under Ψ of elements of $\ker\widetilde{\Psi}$. The map Φ is constructed so that its image is the kernel of Ψ; in other words L is the (first) syzygy module of $(h_1, \ldots, h_n)$. It was Schreyer's insight that including the syzygy module L considerably simplifies the proof of the main result in Gröbner basis theory. By making the maps Ψ and Φ explicit it is easy to abstract from the ideal structure, and apply the same idea to other algebraic structures. In essence, this is the idea of the standard map approach.

1.3 Discussion

We present a discussion on our results and methods.

1.3.1 Discussion – reduction methods

In the previous sections the application of both the planar reduction (PR) method and the energy–momentum (EM) method to the spring–pendulum in $1 : 2$ resonance has been summarized. At this point therefore, we may try to compare both methods.

Both methods arrive at precisely the same asymptotic expansion of the bifurcation curve for the Hamiltonian pitchfork bifurcation, (1.6) and (1.9), which also agrees well with the numerical results of table 2.2, Sect. 2.3.3.

The polynomial normal forms the methods arrive at are rather different. The PR method arrives at a homogeneous third order polynomial as planar Hamiltonian, which was easy to analyze. In contrast, the energy–momentum

method yielded a map with a quadratic and a quartic polynomial as components. This model has a more complicated bifurcation structure than the planar model. However, as stated before, the additional bifurcation (a saddle–node bifurcation) occurs away from the origin in parameter space.

Besides yielding a simpler model, the calculations associated to the PR method are simpler than those of the EM method, because the former employs (equivariant) right-transformations as equivalences in the second reduction stage, resulting in a tangent space with an ideal structure. The EM method also uses left-transformations, yielding a much more complicated tangent space. Technical complications also arise from the additional reduction step, used for reducing from a tangent space of maps to $\mathbb{R}^2$, to one of functions to $\mathbb{R}$. The de-reduction step necessary when computing the reparametrization explicitly is not needed for the PR method. Finally, the more general transformations allowed in the EM method deform the H_2-level sets and require calculation of the inverse transformation, in order for the bifurcation curve to be found (see Sect. 3.4.3).

The EM method is able to handle any resonance. In Chap. 3 the 1 : 2 resonance is analyzed in detail, and some calculations for the 1 : 3 and 1 : 4 case have also been done. The PR method is less suited for analyzing resonances with odd denominator, because square roots turn up in an essential way. In addition, the symmetry resulting from the Birkhoff normalization is not fully exploited, leading to a higher codimension. Indeed, for the 1 : 4 resonance it is already infinitely high. Interestingly, for the 1 : 2 case the codimensions are equal for both reduction methods.

The PR method, and especially the final BCKV normal form, seems better suited to de-reduction to the full phase space than the EM method. The reason is that the latter mixes the integral of motion H_2 with the Hamiltonian H in the left-transformations on the energy–momentum map, whereas BCKV-restricted morphisms do not. For the organization of Hamiltonian level sets on levels of H_2 this makes no difference. It does necessitate an additional computation to pull back the bifurcation curves in terms of H_2. Perhaps more importantly, if one is interested in the organization of the Hamiltonian's level sets in the full phase space, the extra transformations need to be taken into account when drawing conclusions for the real system from the model.

1.3.2 Discussion – standard bases

Standard bases arose in the course of our research, as a natural way to bring several very similar results on common denominator. The result was a unifying proof of the basic results on Gröbner bases, based on a proof due to Schreyer and Greuel, which lent itself immediately to the necessary generalizations.

We almost always work in the ring of truncated formal power series. Results for the formal power series ring are also given (see Sect. 6.5), and involve only an existence proof of the normal form map in this context. We give some remarks on the case of the rational function ring, where Mora's algorithm takes the place of the normal form map. The structures we apply the standard map approach to,

are ideals, modules and algebras, for which the results are already well-known. For example, what we call standard bases for algebras are known as *canonical subalgebra bases* or *SAGBI bases* in the literature. Our main application, standard bases for left–right tangent spaces, is surely new. It should be easy to adapt the approach to other situations as well.

For example, the tangent space used by Golubitsky and Schaeffer [GS85] of unfoldings $g(x, \lambda)$, where $x \in \mathbb{R}$ and $\lambda \in \mathbb{R}$, consists of all germs of the form

$$(1.10) \qquad a(x, \lambda)g + b(x, \lambda)\frac{\partial g}{\partial x} + c(\lambda)\frac{\partial g}{\partial \lambda}.$$

Here a, b, c are arbitrary functions, and note that c does not depend on x. Because of this, this tangent space is not an ideal in the ring of functions in x, λ. In [GS85], the codimension of the vector space (1.10) is computed by noting that one may restrict to the space of truncated formal power series, for a suitable truncation degree, reducing the question to linear algebra. The standard map approach is a systematic and efficient method for solving this linear algebra problem.

1.4 Outline

This work is split into two parts. In Part I we discuss the two reduction methods for Hamiltonian systems considered here, and apply the algorithmic methods to compute exact bifurcation curves in original coordinates, comparing these with numerically obtained phase pictures. The dynamical system we consider is a two-degree-of-freedom spring–pendulum around $1:2$ resonance. We decided to focus on one specific system, around a single resonance that can be analyzed by both methods, in order to make comparisons. The methods are general, however, and throughout generality is retained in the formulations as much as possible.

After these applications, the theory behind these computations is developed in Part II. Much well-known material is summarized in some detail, such as Hamiltonian mechanics, Birkhoff normal forms and singularity theory. We retain an algorithmic focus throughout, but especially in Chap. 4 about Birkhoff normal forms, and Chaps. 6 and 7 about Kas and Schlessinger's algorithm and the infinitesimal stability equation. We now give a short overview for each chapter.

Chapter 2 deals with the planar reduction method, involving first Birkhoff normalization, then a symmetry reduction to the plane using the $\mathbb{S}^1$ normal form symmetry, and subsequently planar $\mathbb{Z}_2$-equivariant singularity theory. A versal model of the planar unfolding is computed, with its bifurcation curves, which are pulled back to the original parameter space and compared to numerical results. Basically, this follows our paper [BHLV98].

Chapter 3 deals with the energy–momentum map method. This too starts with a Birkhoff normalization, but then it immediately applies singularity theory to the energy–momentum map, with equivalences defined by left–right transformations. Again a versal model is computed, its bifurcation diagram pulled back, and results compared to numerical pictures.

Chapter 4 summarizes some Hamiltonian mechanics and the Birkhoff normal form. We quote Birkhoff's original result, as well as more modern version which allows normalization around resonances. In line with the algorithmic emphasis we make a comparison between several algorithms for calculating the Birkhoff normal form, and propose one of our own.

Chapter 5 introduces the necessary singularity theory. As explained before, we use both right-transformations as well as left–right transformations. To explain the ideas we first give the finite-dimensional version, with a smooth Lie group acting on a smooth manifold. Then we quote analogous results for the case of smooth reparametrizations acting on function spaces, where technical complications show up that necessitate the use of the Mather–Malgrange preparation theorem. In this chapter we prove some smooth results, but this is not given great emphasis as in the applications we always use truncated formal power series. However, the results are important in order to show these finite expansions are indeed the 'shadow' or 'projection' or something 'really out there' in the form of smooth transformations.

Chapter 6 develops the standard map approach to Gröbner bases. Motivation for this approach has been given in this introduction, and is provided by Chap. 7 which applies the results obtained here. The chapter starts with a quick overview of Gröbner basis, in a slightly different perspective facilitating the step to more general situations. We proceed to give the abstract underpinnings of the standard map approach, listing the properties and constructions involved, and proving the standard map theorem 6.10. We proceed to prove the basic facts of Gröbner bases using this approach, and doing the same for canonical subalgebra bases and a few others, culminating in the standard basis theorem for left–right tangent spaces as used in the energy–momentum reduction method.

Chapter 7 shows how to combine Kas and Schlessinger's algorithm and the results from the previous chapter to perform the calculations of Chaps. 2 and 3. For the planar reduction method this is straightforward, and has been published in [BHLV98]. The complications for the energy–momentum reduction method are twofold. Most of the complications are related to the algebraic structure of the left–right tangent space, and are dealt with in Chap. 6. The other complication is technical in nature: The calculation of the tangent space involves a reduction from maps to $\mathbb{R}^2$ to functions, and to complete the calculation this reduction has to be undone. This involves reading the story of Chap. 3 backwards, and results in a long calculation.